Geophysical Journal International

*Geophys. J. Int.* (2013) **193,** 1239–1249
Advance Access publication 2013 April 01

doi: 10.1093/gji/ggt078

# The effect of cooling rate on the intensity of thermoremanent magnetization (TRM) acquired by assemblages of pseudo-single domain, multidomain and interacting single-domain grains

A. J. Biggin,[1] S. Badejo,[1] E. Hodgson,[1] A. R. Muxworthy,[2] J. Shaw[1] and M. J. Dekkers[3]

[1] *Geomagnetism Laboratory, Department of Earth, Ocean and Ecological Sciences, University of Liverpool, Oliver Lodge Laboratories, Liverpool L69 7ZE, UK. E-mail: A.Biggin@liverpool.ac.uk*
[2] *Department of Earth Science & Engineering, Imperial College London, South Kensington Campus, London SW7 2AZ, UK*
[3] *Paleomagnetic Laboratory Fort Hoofddijk, Utrecht University, Budapestlaan 17, 3584 CD Utrecht, The Netherlands*

Accepted 2013 February 22. Received 2013 February 21; in original form 2012 November 22

## SUMMARY

Experiments designed to measure the absolute palaeointensity of the geomagnetic field generally do so by comparing the ancient thermoremanent magnetization (TRM) retained by an igneous rock with a new TRM imparted in the laboratory. One problem with this procedure is that the relative magnitudes of the ancient and laboratory TRMs may be influenced, not only by the external field intensities at the time the two coolings took place, but also by the rate at which the coolings themselves occurred. Here, we present new measurements of this 'cooling rate effect' obtained from treatments in the laboratory differing in cooling rate by a factor of ∼200. Synthetic samples containing sized ferrimagnetic grains were used in the experiments. Theoretical considerations and previous experiments have indicated the cooling rate effect to be dependent on domain state. Increases in TRM magnitude of more than 7 per cent per order of magnitude decrease in cooling rate have been reported for assemblages of non-interacting single-domain (SD) grains. Here, we focus on magnetite grains in the less well-studied pseudo-single domain (PSD) and multidomain (MD) states using a range of applied field intensities to impart the TRMs. For the first time, we also measure the cooling rate effect in grains of titanomagnetite that have been oxyexsolved so that they contain strongly interacting SD lamellae. In all cases, the cooling rate effect measured was in the same sense as already observed in ideal magnetically non-interacting SD grains but was considerably weaker. On average, the effect did not exceed ∼3 per cent increase in TRM per order of magnitude decrease in cooling rate and did not show any systematic dependence on applied field intensity. In some samples containing coarser grains, the cooling rate effect was not distinguishable from zero. The sense and magnitude of the cooling rate effect remain uncertain in truly MD grains as different studies have produced discrepant results. For the more practically relevant case of PSD and interacting SD grains, which commonly dominate the TRM in igneous rocks, however, it appears that we can be more confident in our assertions. The cooling rate effect in such materials is in the same sense as in non-interacting SD grains but smaller: a consequence of long-range ordering. In lavas and small intrusions containing these, it is unlikely to exceed 10 per cent. Although a correction should always be attempted, the results of palaeointensity studies based upon such samples will generally not be severely biased.

**Key words:** Archaeomagnetism; Palaeointensity; Rock and mineral magnetism.

## 1 INTRODUCTION

Thermoremanent magnetization (TRM) is acquired by any ferromagnetic material that cools down from above its Curie temperature in the presence of a magnetic field. Being the dominant type of remanent magnetization acquired by igneous rocks as they form, TRMs are ubiquitous in nature and rocks bearing such magnetizations are commonly studied by palaeomagnetists. Although palaeomagnetic directions or 'relative palaeointensities' may be recovered from samples recording various types of remanent magnetization, TRM alone is suitable for the measurement of the 'absolute palaeointensity'. This is because it is the only type of primary magnetization that can readily be reproduced in the laboratory. This, together with the linear relation between TRM and the imparting field's intensity

for weak fields like the Earth's, allows the ratio of the laboratory and natural TRMs to be used to determine the ancient field intensity, that is, (Folgerhaiter 1899);

$$\frac{TRM_{\text{natural}}}{TRM_{\text{lab}}} = \frac{H_{\text{ancient}}}{H_{\text{lab}}}, \tag{1}$$

where $TRM_{\text{natural}}$ and $TRM_{\text{lab}}$ are the natural and laboratory magnetizations acquired in fields $H_{\text{ancient}}$ and $H_{\text{lab}}$, respectively.

Though it is the pillar-stone of palaeointensity determination, eq. (1) only strictly holds true if the rates of cooling during which the two TRMs were acquired are identical. This is generally not the case, however. In both nature and the laboratory, the cooling is generally close to Newtonian and therefore follows an exponential rate with time but the magnitude of this rate may differ by many orders. Igneous rock units frequently have a thickness of metres to kilometres producing a much slower natural cooling than centimetre-sized samples subject to active fan-assisted cooling. Since the magnitude of the TRMs acquired under the different conditions are each also a function of these rates, we have

$$H_{\text{ancient}} = f_{CR}\frac{TRM_{\text{natural}}}{TRM_{\text{lab}}} \cdot H_{\text{lab}}, \tag{2}$$

where the cooling rate correction factor

$$f_{CR} = \frac{1}{1+\Delta TRM}, \tag{3}$$

and the fraction of palaeointensity over- or underestimate

$$\Delta TRM = k \cdot \log\left(\frac{CR_{\text{lab}}}{CR_{\text{natural}}}\right), \tag{4}$$

where $CR_{\text{lab}}/CR_{\text{natural}}$ is the ratio of the cooling rates (or the inverse ratio of the cooling times) between two temperatures on which the cooling rate effect depends logarithmically (Papusoi 1972a; Dodson & McClelland-Brown 1980; Halgedahl *et al.* 1980). The constant $k$ defines the magnitude and sign of the cooling rate effect and is a function of the sample properties. Fig. 1 summarizes the results of some previous studies (Fox & Aitken 1980; McClelland-Brown 1984; Ferk *et al.* 2010; Yu 2011) which have attempted to measure $\Delta TRM$ directly or calculate $k$ (the slope of a line passing through the origin of this plot) from theory.

It is well established from both theory (Dodson & McClelland-Brown 1980; Halgedahl *et al.* 1980) and experiment (Fox & Aitken 1980; Leonhardt *et al.* 2006; Morales *et al.* 2006) that in the case of an assemblage of 'ideal' non-interacting single-domain (SD) grains, $k$ is positive. This leads, in the normal situation of $CR_{\text{lab}} > CR_{\text{natural}}$, to the palaeointensity being overestimated (i.e. $\Delta TRM$ is positive) if an appropriate correction is not made. This is intuitive from Néel (1955) theory: a slower cooling rate leads to the sample spending longer at any given temperature allowing more domain states to populate the higher magnetization state. Using a stepwise approximation for the measurement time, Halgedahl *et al.* (1980) theoretically determined this effect to be approximately 5 per cent per order of magnitude difference in the cooling rates. In contrast, using a rate-dependent function for the measurement time, Muxworthy *et al.* (2011) determined a value of ~8 per cent. Experimentally, values of ~7 per cent per order of magnitude and somewhat variable have been observed (e.g. Papusoi 1972a; McClelland-Brown 1984; Ferk *et al.* 2010, Fig. 1). Theory and observation support that, even in the ideal case of non-interacting SD grains, the cooling rate effect is rather sensitive to the precise distribution of grain sizes and shapes leading to substantial variations in its magnitude (Halgedahl *et al.* 1980; Winklhofer *et al.* 1997; Ferk *et al.* 2010). Furthermore, Yu (2011) demonstrated that the effect is less

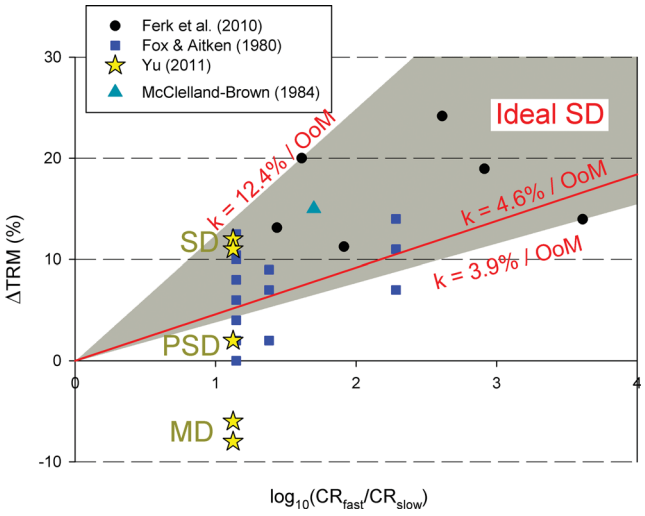


**Figure 1.** Summary plot of cooling rate effect measured in some previous studies. The domain states of samples measured by Ferk *et al.* (2010) and McClelland-Brown (1984) were near-SD; those of Yu (2011) were variable as shown; those of Fox & Aitken's ceramics were not defined (but probably SD to PSD). The red envelope defines the limits of the effect as measured in samples believed to contain non-interacting SD grains. The red line shows the theoretical average effect estimated from theory for uniaxial non-interacting SD grains with coherent rotation of spins (Halgedahl *et al.* 1980). OoM, order of magnitude. Experimental results were only included in this figure where the relevant data were supplied in tables instead of, or in addition to, in plots.

significant at higher than at lower blocking temperatures. This could be an important detail for Thellier palaeointensity experiments as it can cause the points on an Arai plot to sag below the ideal line at low temperatures worsening the overestimate if this portion alone is used (Yu 2011).

$TRM_{\text{lab}}$ is generally imparted over as short a time as possible to reduce the duration of the lengthy palaeointensity protocols as far as practical. Cooling times for most thermal demagnetizers are generally between 10 min and several hours from above the Curie temperature of magnetite (580 °C). The use of minisamples can reduce this to as low as a minute whereas controlled atmosphere ovens can take nearly a day for a single treatment. The slower of these rates may be approximately equivalent to typical rates for archaeological materials that have generally acquired their TRM in a kiln or furnace. By contrast, with the exception of the quenched glassy margins of some lavas, cooling times for $TRM_{\text{ancient}}$ acquired in rocks are typically much longer: at least several days but extending to millions of years for rocks derived from large batholiths. Consequently, the difference in cooling rates could exceed 10 orders of magnitude which would produce overestimates of the palaeointensity approaching the 100 per cent mark. Non-interacting SD grains are not anticipated to be common carriers of TRM in large intrusions; however, because the slow cooling will favour larger grain sizes. Indeed, few natural materials retain their TRMs in assemblages of non-interacting SD grains. Those materials that are closest to this ideal situation (archaeological materials and volcanic glass), moreover, will have cooled the fastest in any case. The vast majority of palaeomagnetic recorders is coarser grained and contain less ideal carriers of TRM for which the cooling rate effect is less well described.

Typical palaeomagnetic recorders in lavas and intrusions are titanomagnetite or magnetite grains spanning a range of sizes from SD to pseudo-single domain (PSD) and multidomain (MD). The influence of cooling rate on TRM intensity recorded in assemblages

of these larger grains is less well constrained by both theory and experiment. Because of self-demagnetization and transdomain processes (Dunlop *et al.* 1994; Muxworthy *et al.* 2003), it is thought likely that $k$ has a negative sign in MD grains such that slower cooling leads to weaker TRMs being imparted (McClelland-Brown 1984; Winklhofer *et al.* 1997; Muxworthy & Heslop 2011). There is some experimental support for this claim (Papusoi 1972b; Yu 2011) with the cooling rate effect observed to be smaller and of reversed sign in samples containing uniquely MD grains and being close to zero in assemblage of PSD-sized grains (Fig. 1).

Commonly in igneous rocks sampled for palaeomagnetic studies, large grains of titanomagnetite have undergone a process of oxyexsolution to produce lamellae of near-stoichiometric magnetite interspersed with non-magnetic near-ilmenite (Dunlop & Özdemir 1997). The result is that large homogeneous ferrimagnetic grains have effectively been replaced with assemblages of magnetically interacting SD grains. Such assemblages of interacting grains can form 'magnetic superstates' whereby they collectively exhibit structures (e.g. vortex or MD) akin to large single grains (Harrison *et al.* 2002).

Despite their rather common occurrence in nature and consequent importance for palaeomagnetism, little work has been carried out to explicitly investigate the TRM characteristics of assemblages of interacting lamellae of near-stoichiometric magnetite. To date, no experimental study has been undertaken to observe the effects of variable cooling rates on TRM intensity in samples containing such grains.

The thermally activated Preisach model for assemblages of uniaxial SD grains by Stancu & Spinu (1998), was extended by Muxworthy & Heslop (2011), to examine the cooling rate effect of TRM acquisition. This model accommodates intergrain magnetostatic interactions, and predicts that such interactions severely dampen the cooling rate effect causing it to reverse sign (Muxworthy *et al.* 2011) so that slower cooling produces marginally weaker TRMs. This has not yet been confirmed experimentally.

The present uncertainty surrounding the nature of the cooling rate effect in samples containing grains other than non-interacting SD ferrimagnetic grains remains a major limiting factor in the confidence we can place in palaeointensity determinations. Cooling rate corrections are much more frequently measured and applied in archaeointensity than in palaeointensity studies. This is, in part, because the measurement of a reliable correction requires that the sample be heated above its Curie temperature while undergoing no magnetic alteration: a criterion that many rocks cannot meet. It is also because the cooling rate effect has not yet been demonstrated to be problematic in TRM carriers typical found in igneous rocks. Nevertheless, the present lack of evidence one way or the other forces many studies to acknowledge a potential uncertainty in their results frequently amounting to several tens of per cent (e.g. Tarduno *et al.* 2010).

This study experimentally investigated the effect of cooling rate on the TRM intensities acquired by a selection of synthetic samples containing PSD, MD and interacting SD grains of near-stoichiometric magnetite. It additionally explored whether there is any field dependence of the cooling rate effect.

## 2 SAMPLES AND METHODOLOGY

### 2.1 Samples and rock magnetic characterization

The majority of samples used were prepared for the purpose of this study using existing ferrimagnetic powders of four types.

Powders HM4 and LM6 both consist of crushed natural material that had been sieved into sized fractions ranging from $<5$ to $>250$ μm. These were originally studied by Hartstra (1982a,b, 1983) who characterized then with optical microscope, X-ray diffraction and microprobe analysis and subsequently investigated their bulk magnetic properties and the characteristics of different types of remanence (isothermal, anhysteretic and thermal) held by them.

HM4 is a crushed homogeneous magnetite and LM6 is a titanomagnetite that has undergone oxyexsolution to produce lamellae of Al-substituted near-stoichiometric magnetite (magnetite with a small hercynite fraction) and ilmenite. These lamellae are occasionally as wide as 5 μm but much finer lamellae are also abundant so that, irrespective of the bulk grain size, the LM6 material is essentially subdivided into interacting SD grains.

WA and WB samples are magnetic pigments provided by Wright Industries with the serial codes 031182 and 082800, respectively. The nominal description given for WA is that it is pure magnetite with a mean grain size of 0.7 μm. No prior information was available for WB but it appears finer (i.e. $<0.5$ μm) under reflected light and thermomagnetic analysis (see Section 3.1) suggested somewhat oxidized magnetite.

These powders were dispersed in NaCl in a concentration of 0.5 per cent and pressed into cylindrical pellets of diameter and length 10 mm before being sealed, under vacuum, in quartz capsules.

A number of samples prepared by Dankers (1981), were also used in this study. These D samples contained powders of crushed and sized homogeneous natural magnetite mixed with KBr powder at a concentration of 2–3 per cent, pressed into ∼5 mm pellets and placed within evacuated quartz capsules (McClelland & Shcherbakov 1995). Scanning electron microscope (SEM) analysis by McClelland & Shcherbakov (1995) confirmed the stated grain size fractions are correct to within 10 per cent; no fine adhering particles were observed.

A total of 18 samples were used in this study and these were produced using the 15 powders listed in Table 1 alongside some of their measured rock magnetic properties. Isothermal remanent magnetization (IRM) acquisition, hysteresis, IRM backfield, first-order reversal curve (FORC) diagrams and thermomagnetic measurements were made using a Magnetic Measurements Ltd (Aughton, Lancashire, UK) variable field translation balance (VFTB) and a Princeton Measurements Corp (Westerville, OH, USA) alternating gradient magnetometer (AGM) and vibrating sample magnetometer (VSM). These rock magnetic experiments were undertaken in the order given above using material from pellets that had not yet been heated.

### 2.2 Cooling rate experiments

Prior to the cooling rate experiments, all encapsulated samples were heated to 700 °C and held for 30 min to stabilize their magnetic properties against further heatings (to maximum 600 °C) and to reduce the internal stress of the grains. These specific samples were then characterized by performing stepwise thermal demagnetization of a full TRM and then by measuring the size of the high-temperature 'tail' (Bol'shakov & Shcherbakova 1979) of a partial TRM. This pTRM was imparted by applying a field of 80 μT while the fully demagnetized samples were heated from room temperature $T_r$ to 520 °C and then cooled back to $T_r$ (it is therefore a pTRMc by the definition of Biggin & Poidras 2006). The tail of this pTRM was then measured after a further identical thermal treatment undertaken in zero applied field. Its size relative to the pTRM

**Table 1.** Rock magnetic properties of samples used in this study. * indicates an average of values from two specimens in the cases of HM4 5–10, LM < 5, and LM6 150–250.

| Name (grain size in μm) | Mineralogy | $M_s$ ($Am^2\ kg^{-1}$) | $M_{rs}$ ($Am^2\ kg^{-1}$) | $H_c$ (mT) | $H_{cr}/H_c$ | $M_{rs}/M_s$ | Curie Temp | Tail [$pTRM_{520,0}$]* (per cent) |
|---|---|---|---|---|---|---|---|---|
| WB < 0.5 | magnetite | 0.11 | 0.010 | 9.13 | 3.52 | 0.095 | 574, 623 | 20 |
| WA 0.7 | magnetite | 0.55 | 0.158 | 33.94 | 1.69 | 0.288 | 577 | 23 |
| HM4 5–10 | magnetite | 0.44 | 0.029 | 7.60 | 4.05 | 0.066 | 577 | 24 |
| HM4 15–20 | Magnetite | 0.26 | 0.009 | 4.32 | 6.01 | 0.034 | 577 | 16 |
| HM4 25–30 | Magnetite | 0.18 | 0.005 | 3.90 | 6.66 | 0.030 | 579 | 20 |
| HM4 40–55 | Magnetite | 0.28 | 0.005 | 2.27 | 12.03 | 0.017 | 581 | 29 |
| HM4 55–75 | Magnetite | 0.66 | 0.013 | 2.67 | 8.54 | 0.020 | 580 | 19 |
| HM4 75–100 | Magnetite | 0.57 | 0.011 | 2.81 | 9.72 | 0.020 | 578 | 20 |
| LM6 < 5 | Oxyexsolved TM | 0.22 | 0.041 | 23.19 | 2.13 | 0.183 | 569 | 6 |
| LM6 25–30 | Oxyexsolved TM | 0.44 | 0.034 | 9.91 | 3.44 | 0.076 | 567 | 17 |
| LM6 75–100 | Oxyexsolved TM | 0.94 | 0.057 | 8.44 | 4.01 | 0.061 | 569 | 21 |
| LM6 150–250 | Oxyexsolved TM | 0.23 | 0.017 | 8.10 | 3.17 | 0.072 | ∼580 | 25 |
| D 15–20 | Magnetite | | | 5.8 | 3.66 | 0.065 | 580 | 8 |
| D 20–25 | Magnetite | | | 4.1 | 4.39 | 0.044 | 580 | 8 |
| D 25–30 | Magnetite | | | 3.3 | 5.79 | 0.032 | 580 | 12 |

itself is a measure of the extent to which Thellier's (1938) law of reciprocity is violated. This law states that a pTRM imparted between two blocking temperatures should be demagnetized entirely in the same range and is only strictly adhered to by non-interacting SD grains (see, e.g. Dunlop & Özdemir 2001).

The cooling rate experiments themselves were undertaken at the University of Liverpool. They consisted of the imparting of TRMs to the encapsulated samples (listed in Table 2) by cooling them from 600 °C to $T_r$ in an applied constant field using two different ovens with very different cooling rates. Each sample was subjected to a series of paired fast and slow treatments using at least three different applied field intensities in the range 30–180 μT. The use of these different field intensities allowed checks for the reproducibility of any cooling rate effect to be made alongside tests for the linearity of the different types of TRM in this field range.

For fast cooling rate experiments (FAST), a Magnetic Measurements thermal demagnetizer (MMTD) with cooling fan was used, whereas for 'slow' cooling rate experiments (SLOW) a custom-built oven with thick thermal insulation and no fan was used. Plots of the cooling profiles from these two ovens are given in Fig. 2 which shows that they are very similar in shape and therefore have a nearly constant cooling rate ratio over practically the full temperature range. This ratio is approximately 200 and the shape of both curves is close to exponential decay as expected for natural Newtonian cooling. The average cooling rates over the temperature interval 580–50 °C were 77.7 °C $min^{-1}$ (1.3 °C $s^{-1}$) for FAST and 0.4 °C $min^{-1}$ for SLOW. Although the slow cool oven took only approximately 24 hr to cool to 50 °C, the samples were generally left in it, with the field applied, for at least a further 24 hr while they equilibrated to room temperature.

A great deal of care was taken to ensure equivalence in everything except cooling rate in all heating–cooling cycles. The field was carefully mapped inside both ovens for every current setting applied, the same single sample holder was transferred from oven to oven and used for every treatment and samples were kept in the same positions relative to one another. Similarly, at the end of every thermal treatment, the samples were kept in zero field inside the oven for at least 30 min and then kept in zero field outside of the oven for the same period prior to being measured. This was done to minimize the effects of short-timescale viscous magnetizations that could introduce additional noise into the measurements. One batch of samples was additionally thermally demagnetized to a peak temperature of 100 °C in the fast oven subsequent to every full TRM treatment (imparted in both the fast and slow ovens). This was done to check the extent to which the lowest blocking temperature portions of samples' remanences were influencing the two different types of TRM.

As a check on the outcome of the main experiments, in particular to ensure that no overlooked intrinsic difference between the two ovens was influencing the results, two further treatments were applied to a selection of samples. Unlike the main experiments, these were undertaken in a single high-precision Magnetic Measurements Ltd oven capable of variable cooling rates. These treatments consisted of full TRMs imparted in an applied field of 75 μT using cooling times of 30 and 255 min from 600 to 50 °C (average cooling rates of 18.3 and 2.2 °C $min^{-1}$).

Measurements of the magnetization in all cases were made using a Tristan Technologies (San Diego, CA, USA) three-axis SQUID system. Measurements of the moments made after the initial 700 °C demagnetization were subtracted from all subsequent measurements to remove any induced component. In addition, empty holder measurements were made at the beginning and end of each measuring session to provide a correction for the holder and for any drift of the instrument (although the latter was found to be negligible).

Repeated full TRM treatments made using the FAST oven and the same applied field in each case were used as checks for magnetic alteration of the samples. Each sample was subject to at least three of these including one at the start and the end of the full experimental run. Accepted samples were required to produce check measurements that were repeatable to within 5 per cent and show no progressive trend through the experiments; the majority of checks were repeatable to within 2 per cent (see Table 2).

## 3 RESULTS

### 3.1 Results of the rock magnetic experiments

Example plots of each type of experiment are given in Figs 3 and 4 and the results are summarized in Table 1. As expected, IRM acquisition plots uniquely saturated at low fields (<300 mT) and hysteresis parameters tended to show a clear relationship with grain size (Fig. 5). The sample WB < 0.5 with nominally the finest grain size fraction surprisingly showed hysteresis parameters indicative of coarse PSD to MD properties. To test whether this could be due to a superparamagnetic fraction, we measured the bulk susceptibility of the encapsulated and heated sample at three frequencies (976, 3904 and 15 616 Hz) using an AGICO KLY4S kappa bridge. We found

**Table 2.** Summary of cooling rate effects illustrated in figure D. Shaded italicized results are those from samples with standard deviations > 5 per cent. Individual results marked with * were excluded as outliers (see text). Min. Reproducibility refers to the highest absolute levels of variation found between the alteration checks. Stabilization refers to the change in TRM intensity caused by the initial heating to 700 °C. Results in parentheses are those found after applying partial thermal demagnetization treatments to 100 °C after both SLOW and FAST TRM acquisition treatments.

| | | | Δ*TRM* (per cent) | | | | | | | |
|---|---|---|---|---|---|---|---|---|---|---|
| Sample | Min. Reproducibility (per cent) | Stabilization (per cent) | 30 μT | 60 μT | 80 μT | 100 μT | 180 μT | Mean | 95 per cent conf | *SD* |
| WB <0.5 | −4.8 | 10.2 | | 10.2 (10.0) | | 4.8 (6.2) | 4.5 (4.6) | 6.5 (7.0) | 3.6 (3.2) | 3.2 (2.8) |
| WA 0.7 | 1.6 | −14.4 | 10.4 | 4.6 | 1.7 | 6.6 | | 5.8 | 3.6 | 3.7 |
| HM4 5–10 (1) | 1.0 | −14.1 | 3.2 | 3.3 | −1.3 | 3.3 | | 2.1 | 2.2 | 2.3 |
| *HM4 5–10 (2)* | *−1.4* | *−13.7* | | *10.1 (9.4)* | | *18.7 (11.9)* | *7.1 (7.2)* | *12.0 (9.5)* | *6.8 (2.7)* | *6.0 (2.4)* |
| *D 15–20* | *4.9* | | | *11.4 (2.2)* | | *8.9 (−6.0)* | *1.0 (−5.4)* | *7.1 (−3.1)* | *6.1 (5.2)* | *5.4 (4.6)* |
| HM4 15–20 | 2.2 | −8.6 | −35.1 * | −2.1 | 3.2 | 3.6 | | 1.6 | 3.6 | 3.2 |
| *D 20–25* | *−2.4* | | | *17.6 (9.2)* | *0.9* | *23.6 * (13.6)* | *13.2 (11.6)* | *10.6 (11.5)* | *8.7 (2.5)* | *9.8 (2.2)* |
| HM4 25–30 | −1.0 | −2.6 | 1.1 | 3.2 | 0.5 | 4.0 | | 2.2 | 1.6 | 1.7 |
| *HM4 55–75* | *−1.5* | *10.3* | | *3.8 (−2.4)* | | *26.1 * (6.6)* | *4.6 (0.5)* | *11.5 (1.6)* | *14.4 (5.2)* | *12.7 (4.6)* |
| *HM4 75–100* | *1.5* | *1.1* | *20.8 ** | *5.1* | *−6.3* | *4.4* | | *1.1* | *7.2* | *6.4* |
| | | Magnetite Mean | 4.9 | 6.7 (5.7) | −0.2 | 8.7 (6.5) | 6.1 (3.7) | 5.5 (5.3) | 2.6 (5.2) | 4.2 (6.0) |
| | | Excluding *SD* > 5 per cent | 4.9 | 3.8 | 1.0 | 4.4 | | 3.6 | 2.0 | 2.3 |
| LM6 <5 (1) | −1.6 | −5.8 | 3.5 | 2.8 | | 2.2 | | 2.8 | 0.8 | 0.7 |
| LM6 <5 (2) | 1.1 | 4.9 | 5.0 | 4.3 | 3.7 | 2.8 | | 3.9 | 0.9 | 0.9 |
| LM6 25–30 | 1.0 | −4.0 | 3.2 | 0.1 | −0.3 | 1.0 | | 1.0 | 1.5 | 1.5 |
| LM6 75–100 | −0.6 | −3.7 | 0.4 | 2.5 | | 1.7 | | 1.5 | 1.2 | 1.0 |
| LM6 150–250 (1) | −1.4 | 1.2 | 2.0 | 3.4 | −2.2 | 1.5 | | 1.2 | 2.3 | 2.4 |
| LM6 150–250 (2) | 1.7 | 7.5 | −1.2 | −1.1 | | 1.0 | | −0.5 | 1.4 | 1.2 |
| | | Oxyexsolved TM Mean | 2.2 | 2.0 | 0.4 | 1.7 | | 1.7 | 1.2 | 1.5 |
| | | Grand Mean | 3.1 | 4.9 (5.7) | 0.0 | 5.9 (6.5) | 6.1 (3.7) | 4.6 (5.3) | 2.2 (5.2) | 4.4 (6.0) |
| | | Excluding *SD* > 5 per cent | 3.1 | 2.8 | 0.8 | 2.9 | | 2.6 | 1.2 | 2.1 |

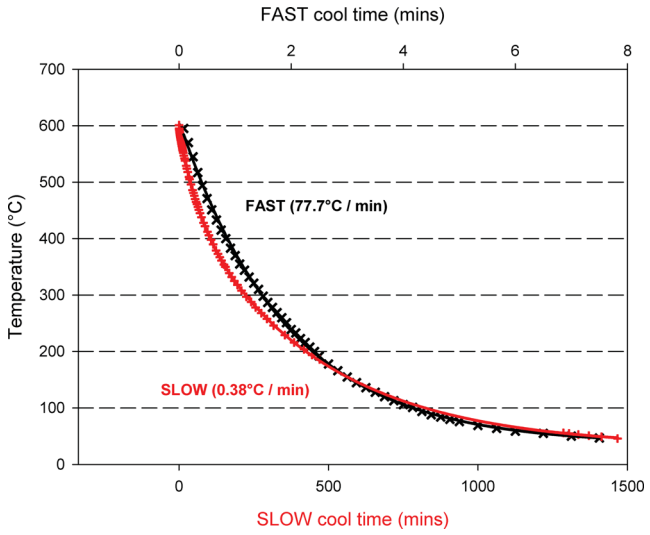


**Figure 2.** Time–temperature profiles for cooling runs in the temperature range 600–50 °C taken from the two ovens used in this study. Two different time axes are used for comparison and the average cooling rates across this temperature range are given.

differences of less than 2.5 per cent across the entire frequency range implying that the superparamagnetic fractions were minimal. The thinner-than-expected hysteresis loops instead suggest that these fine grains were strongly interacting with one another, most likely to be a consequence of clumping together in the pellets.

Many of the powders displayed inflections in the heating curve of the thermomagnetic curves at temperatures in the range of 400–460 °C (Fig. 3) suggesting that they could have undergone some low-temperature oxidation prior to their encapsulation. In this case, the resulting maghemite phase would form a rim around the magnetite grains and would have altered to haematite, which is on the order of 100 times less magnetic, on heating. This could explain some of the decrease in magnetization observed on the cooling curve although, since these heatings were performed in air, high-temperature oxidation of magnetite directly to haematite will also have been widespread. We stress that the alteration observed in the examples in Fig. 3 will have been far more severe than that experienced by the encapsulated sister samples.

FORC diagrams for HM4 samples with grain sizes larger than 15 μm displayed typical MD characteristics with open contours but also a faint high coercivity tail suggestive of a minor haematite phase (Figs 4a and b). FORC diagrams from LM6 samples showed closed contours indicative of SD and PSD behaviour. Sample LM6 <5 μm has a relatively narrow spread in the *y*-axis suggesting that the degree of magnetic interactions is low (Muxworthy *et al.* 2004),

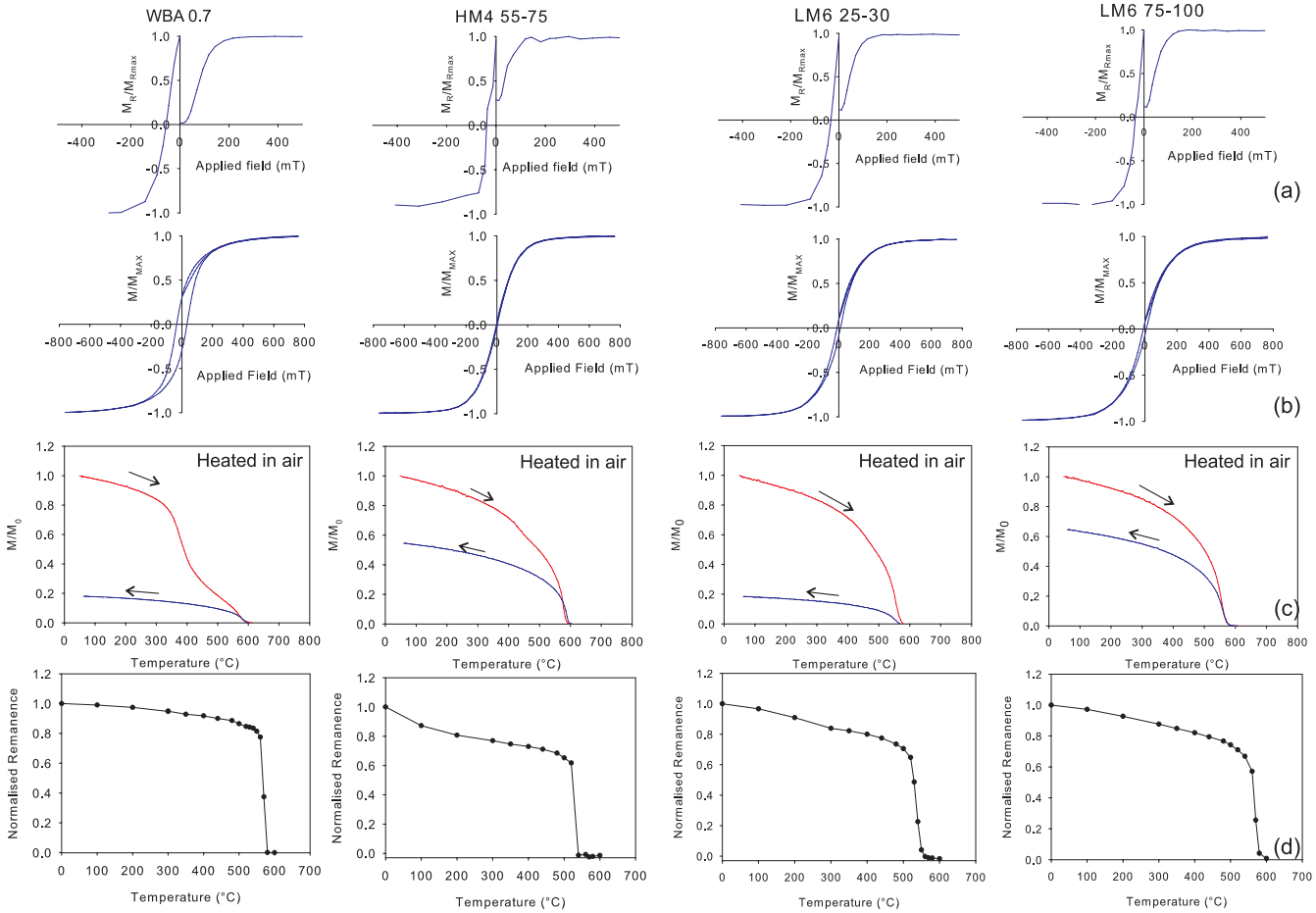


**Figure 3.** Examples of rock magnetic results for four samples (mixtures of powders and salt). For each sample, plots of (a) IRM acquisition and backfield demagnetization, (b) hysteresis loop, (c) high-field thermomagnetic curve (measured in air) and (d) thermal demagnetization of TRM (imparted between 600 °C and $T_r$ in a field of 50 μT) are shown.

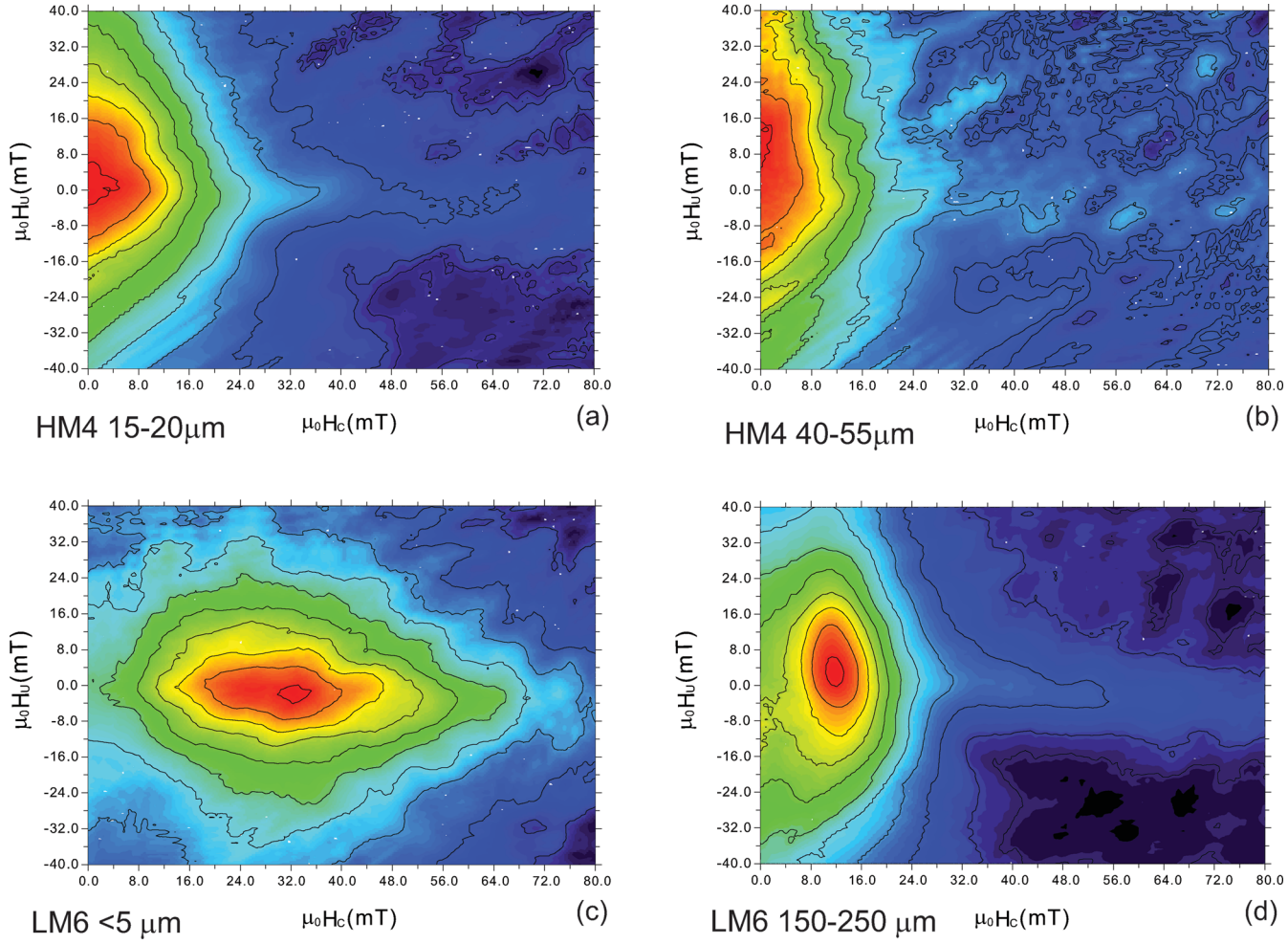


**Figure 4.** FORC diagrams measured for four samples using a smoothing factor of 6 and processed using the in-house Utrecht software written by T. Mullender.

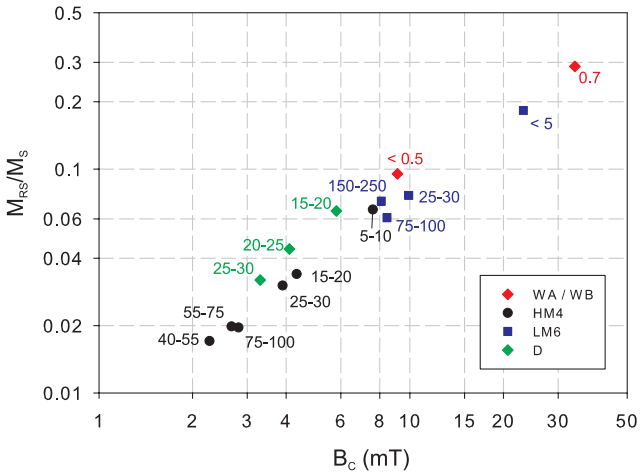


**Figure 5.** Plot of $M_{rs}/M_s$ versus $B_c$ (Tauxe *et al.* 2002) for all samples alongside their grain sizes. Note the log scales on both axes.

in contrast LM6 150–250 μm displays a significantly larger spread in the *y*-axis direction, which is indicative of magnetic interactions. (Figs 4c and d). A high coercivity tail was also evident in the FORC diagram of the LM6 150–250 μm sample.

The measured tails of the pTRMs imparted between 520 °C and $T_r$ were generally substantial (>15 per cent of the pTRMs themselves) but only correlated with grain size for the LM6 samples (Table 1), again suggesting that finer homogeneous grains were clumping together.

No phase other than magnetite was observed in any of the thermomagnetic cooling curves. Furthermore, the stabilized encapsulated samples carrying TRMs imparted in the range 600 °C – $T_r$ were all fully demagnetized by 580 °C. This suggests that the remanence was held primarily by a near-stoichiometric magnetite phase in all of the samples used in the cooling rate experiments although thin rims of haematite may coat the grains in some cases.

### 3.2 Results of the cooling rate experiments

Results from 16 samples are summarized in Fig. 6 and Table 2. For most of these, the linearity of TRM is not substantially violated in the cases of either the SLOW and FAST treatments up to the maximum fields applied (100 or 180 μT). Two exceptions are the samples with the finest grain sizes WA < 0.5 and WB 0.7 which both display markedly lower TRM intensities than expected from linearity with an applied field of 100 μT. In these cases, the SLOW and FAST treatments are similarly affected.

In the majority of samples, the cooling rate effect is small ($\Delta TRM$ is a few per cent) at all field intensities and approaches the noise level observed in the repeat measurements (given in the 'Min. reproducibility' column of Table 2). The large number of samples and measurement steps allows the results to be treated statistically. For all individual samples and/or field intensities, the average $\Delta TRM$ is

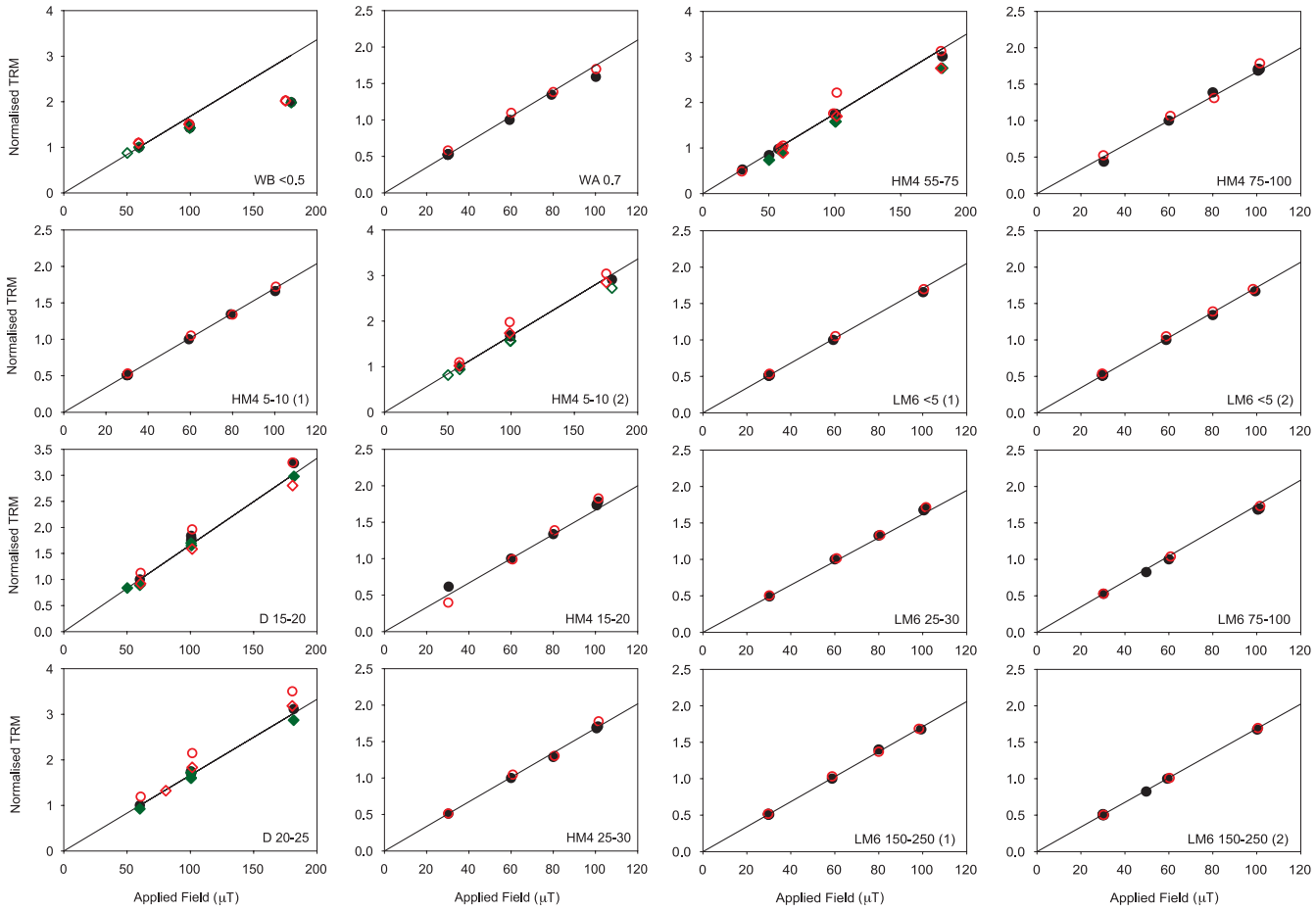


**Figure 6.** Summary of results from all cooling rate experiments shown as plots of TRM intensity versus applied field intensity. Filled black circles pertain to FAST treatments and hollow red circles to SLOW treatments. Filled (green) and unfilled (red) diamonds relate to the measured TRM of FAST and SLOW treatments, respectively, subsequent to a thermal demagnetization treatment to 100 °C.

positive (i.e. the SLOW cooling imparts a stronger TRM than the FAST cooling) or indistinguishable from zero.

The grand mean of $\Delta TRM$ for all samples and all fields is 4.6 ± 2.2 per cent; small but distinguishable from zero. $\Delta TRM$ is larger in the magnetite samples (5.5 ± 2.6 per cent) than in the oxyexsolved titanomagnetite samples (1.7 ± 1.2 per cent) and the difference is significant ($p = 0.019$; two-sample $t$-test); again, both are distinguishable from zero.

In addition to exhibiting stronger cooling rate effects, the magnetite samples also produced greater variations in $\Delta TRM$ with field intensity. The variations are not systematic with the magnitude of the applied field intensity and are therefore not ascribed to genuine dependence of the cooling rate effect on this parameter. Several results were deemed to be outliers by virtue of being at least a factor of 1.5 of the interquartile range outside of the central two quartiles obtained for the entire data set. These are marked with asterisks in Table 2 and were excluded from all calculations. Nevertheless, the cooling rate effect in five magnetite samples (shaded and italicized in Table 2) still produced standard deviations greater than 5 per cent. One of these—HM4 5–10(2)—exhibited far stronger cooling rate effects than its sister sample containing the same magnetite powder. This sample was uniquely positioned in the holder adjacent to and in contact with sample WB < 0.5 which had a magnetization that was a factor of 5 higher than that of any other sample. It is likely that HM4 5–10(2) acquired a stronger TRM in the SLOW treatments as a consequence of this prolonged proximity.

The remainder of samples, both magnetite and oxyexsolved titanomagnetite, displays a broad inverse relationship between their mean cooling rate effect and their grain size (Fig. 7). The mean $\Delta TRM$ for the whole subset with standard deviations less than 5 per cent (2.6 ± 1.2 per cent) is somewhat lower than for the entire data set. The means of the magnetite (3.6 ± 2.0 per cent) and the oxyexsolved titanomagnetite (1.7 ± 1.2 per cent) samples within the subset are somewhat closer to one another though still statistically distinct ($p = 0.032$). It is apparent in this case, however, that it is the two samples with the submicron grain size that are responsible for the observed difference.

The effect of applying a partial thermal demagnetization step to 100 °C (results shown in parentheses in Table 2 and as diamonds in Fig. 6) was generally to make the effects observed for single samples more consistent (i.e. it reduced the individual standard deviations). This suggests that unstable viscous magnetizations were playing some part in producing the observed noise. In some cases (notably D 15–20 and HM4 55–75), it also had the effect of strongly reducing the mean cooling rate effect bringing these more into line with that observed in the other magnetite samples.

## 4 DISCUSSION AND CONCLUSIONS

The observations reported in the previous section and displayed in Figs 6 and 7 and Table 2 can be summarized as

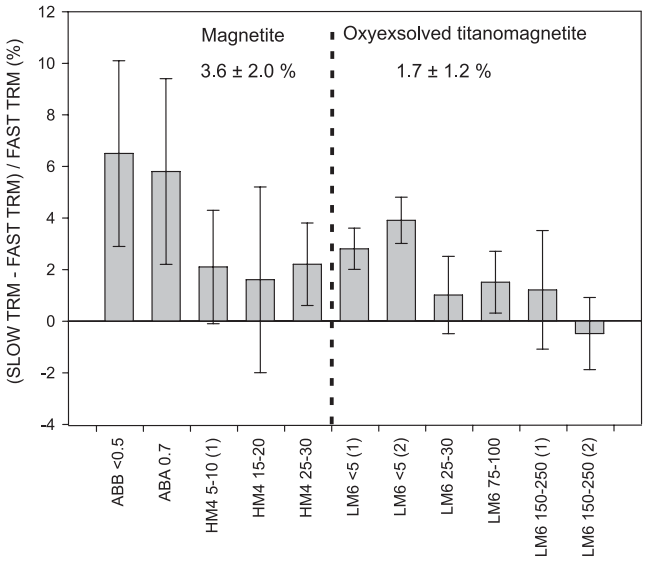


**Figure 7.** Mean cooling rate effect shown with 95 per cent confidence limits for those samples with standard deviation <5 per cent.

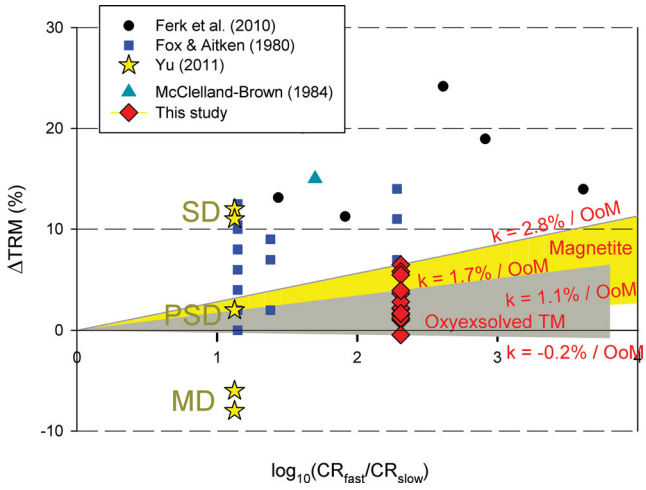


**Figure 8.** Results of this study (red diamonds) plotted alongside some previous results from cooling rate studies (see also Fig. 1). The yellow area brackets the range of $k$ values (given) obtained from the samples containing homogenous magnetite whereas the orange area brackets those from the samples containing oxyexsolved titanomagnetite. OoM, order of magnitude.

– $\Delta TRM$, the effect on TRM intensity produced by a factor ∼200 increase in cooling rates was, on average, small (no more than a few per cent) and positive.

– This effect is strongest in the samples containing the finest (submicron) magnetite powders and is barely distinguishable in samples containing coarser magnetite or oxyexsolved titanomagnetite powders.

– The effect is not notably dependent on the applied field intensity up to 180 μT.

Fig. 8 summarizes the results alongside some of those from earlier studies. The samples containing homogeneous PSD–MD grains bracket values of $k$ between 1.1 and 2.8 per cent per order of magnitude (yellow, lighter shaded area) that encompass the approximate 2 per cent per order of magnitude effect recently obtained by Yu (2011) for both a natural and synthetic (1.06 μm) sample containing PSD grains. Yu's recent study also produced values of $k$ of approximately −6 per cent per order of magnitude for two samples containing MD grains of magnetite (including one synthetic sample with a mean nominal size of 18.3 μm) which are at odds with our results. A third distinct estimate of $k$ for samples containing MD magnetite grains of approximately −2 per cent per order of magnitude (Perrin 1998) was produced by a much older study (Papusoi 1972b). Finally, another recent study (Ferk *et al.* 2012) performed with synthetic samples obtained results broadly in agreement with ours: their values of $k$ for both PSD and MD carriers were positive but tended to be so low (<3 per cent per order of magnitude) as to be indistinguishable from zero.

**Table 3.** Results of additional cooling rate experiments performed using a single oven with $CR_{fast}/CR_{slow} = 8.5$ and $B = 80\ \mu$T.

| Powder | $\Delta TRM$ (per cent) |
|---|---|
| HM4 5–10 | 5.4 |
| HM4 15–20 | 1.8 |
| HM4 25–30 | 8.0 |
| LM6 < 5 | 4.4 |
| LM6 25–30 | 1.1 |
| LM6 150–250 | 1.7 |

Some additional measurements were made late in the study to remove any doubt that our obtained results were due to the fact that two different ovens were used for the two cooling rates. A small collection of samples were given two TRMs (see Section 2.2) in a third oven. This additional data set (Table 3) does not benefit from the repeated treatments of the main set of measurements. Nevertheless, by virtue of containing only positive values of $\Delta TRM$, it is sufficient to verify the reliability of our central findings.

The cause of disagreements in the empirical estimates of the cooling rate effect in pure MD grains observed by this study and Yu (2011) is far from clear but may well lie in subtle differences in the samples used in the different studies. It is acknowledged here that some of the 'magnetite' grains used in this study may have rims of haematite that decrease their effective grain size. Since finer grain sizes are associated with higher values of $k$, it is conceivable that this oxidation could counteract a negative cooling rate effect to an extent sufficient to reverse its sign. This is not an entirely satisfactory explanation, however, given that large departures of these samples from an MD state are not indicated by their hysteresis parameters (Table 1).

### 4.1 Preisach analysis of cooling rate in the oxyexsolved samples

The oxyexsolved titanomagnetite samples produced $k$ values between 1.7 and −0.2 per cent per order of magnitude (orange darker shaded area on Fig. 8), suggesting only a very weak cooling rate effect applies to these types of remanence carriers. In this case, there are no previously published results to compare the data to; we therefore analyse our data using the Preisach model detailed in Muxworthy & Heslop (2011).

It is clear from the FORC diagram shown in Fig. 4(c), that sample LM6 150–250 μm displays a highly interacting, SD/PSD assemblage of grains. We therefore examined this sample in greater detail to examine the role of interactions on the cooling rate. Using the FORC diagram, shown in Fig. 4(c), as input into the model

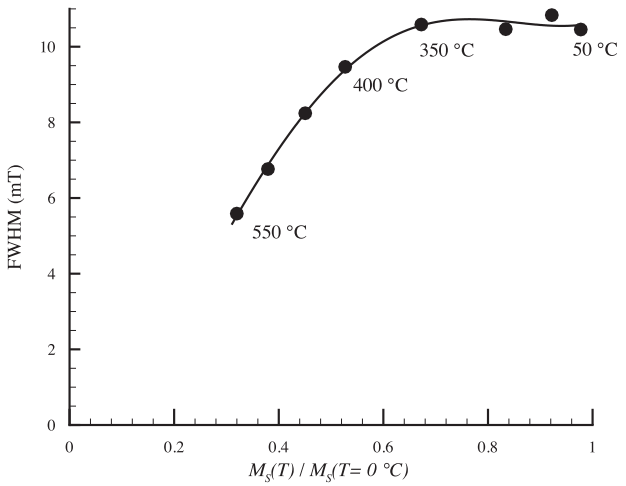


**Figure 9.** Full-width at half maximum (FWHM) versus normalized $M_S(T)$ for sample LM6 150–250 μm, as a function of temperature (50–550 °C). The FWHM was determined by examining the vertical profile through the peak of the FORC distribution as described by Muxworthy & Dunlop (2002). A trend line is depicted.

described in Muxworthy & Heslop (2011), we determined $\Delta TRM$ for cooling rates used in the Section 3.2 and an applied field of 60 μT, yielding a $\Delta TRM \sim -1.0 \pm 0.2$ per cent.

The model of Muxworthy & Heslop (2011) assumes that both the interaction field between grains and the coercive force are $\propto M_S(T)$ (the spontaneous magnetization); this is based on both theoretical arguments and empirical observations (Muxworthy & Dunlop 2002). To rigorously test these assumptions, we tested the thermal dependency of the interaction field distribution and the coercive force as a function of temperature, by measuring FORC diagrams at temperature. As expected, the coercive force was found to be $\propto M_S(T)$ as a first approximation; however, the interaction field, which was quantified using the full width at half maximum (FWHM, Muxworthy & Dunlop 2002), was found not to be $\propto M_S(T)$ (Fig. 9), but instead it displays a distinct deviation and curvature from a linear trend as the temperature is decreased: at high temperature the interaction field appears to be $\propto M_S(T)$, however, at lower temperatures the interaction field no longer increases with $M_S(T)$. Given the highly interacting regime that is thought to exist in the material, it is possible that the curvature marks a break from short-range ordering to long-range ordering, that is, the low-temperature phase is displaying spin-glass behaviour.

Replacing the interaction field relation used in the model of Muxworthy & Heslop (2011), with the data trend shown in Fig. 9, yields a $\Delta TRM \sim 4.0 \pm 0.3$ per cent for the same cooling parameters described earlier, that is, $k$ changes from negative to positive.

### 4.2 Implications for palaeointensity experiments

Table 4 provides guideline estimates for the cooling rate effect in different scenarios based on observed average values of $k$ in Figs 1 and 8. The implications for palaeointensity investigations appear to be broadly reassuring. In the many published studies dealing with lavas or small-scale intrusions where cooling rate corrections were not applied on the basis of the samples containing other than ideal SD grains, the palaeointensity estimates were probably not biased more than 10 per cent by this effect.

Certain previous studies have blamed the cooling rate effect in MD grains for too low palaeointensity measurements obtained from historic lavas ∼20 per cent from Mount Etna (Sicily) (Hill & Shaw 1999; Biggin *et al.* 2007). This would have amounted to a $k$ value of between −2 and −4 per cent per order of magnitude that is not supported by the results obtained here. An alternative explanation in this case has already been put forward (de Groot *et al.* 2012) whereby 'magnetic alteration' occurred during heating and was detectable through ARM acquisition experiments performed as a function of magnetic starting state.

It is pleasing to note that there is an inherent process at work to limit the magnitude of any cooling rate effect. Namely, that those materials containing near-ideal SD grains that are most susceptible to cooling rate biases are also those that most likely cooled fastest in nature (i.e. volcanic glasses, fired pottery, etc.). By contrast, samples from plutons with the largest differences in cooling rate between nature and the laboratory will tend to contain grains that are coarser and potentially oxyexsolved. Similarly, the uncertainty surrounding the sign and magnitude of $k$ applied to pure MD grains may not represent a huge practical limitation because such grains are not commonly expected to be the primary carrier of a stable ancient remanence in rocks. A cooling rate correction is nonetheless required when working with samples containing fine near-ideal SD grains and is also desirable in other cases. This correction should be measured directly wherever possible; the sensitivity of the cooling rate effect to domain state implies that generic guides such as Table 4 are only order of magnitude precise.

Finally, although this study has dealt entirely with full TRMs, it has been empirically demonstrated and stands to reason that the cooling rate effect is also function of blocking temperature (Yu 2011). This implies that the cooling rate effect may differ for partial (pTRMs) and full TRMs potentially introducing an additional source of noise into the results of palaeointensity experiments. A future study will report the results of simulated palaeointensity experiments performed on the synthetic samples studied here; this will use different cooling rates to impart full and partial TRMs.

## ACKNOWLEDGEMENTS

We thank members of the HPT lab and glassblowers at Utrecht University for use of their facilities and expertise in helping to

**Table 4.** Indicative estimates of cooling rate effect on TRM intensity in different sized bodies containing different types of remanence carriers (OoM = order of magnitude). Approximate values of $k$ for ideal SD grains are taken from previous studies (see Fig. 1) whereas the others are based on the findings of this study. A laboratory cooling time of 10 min (appropriate for a medium fan-assisted oven over the temperature range 600–50 °C) and a thermal diffusivity of $10^{-6}$ $m^2/s$ is assumed in all cases.

| Thickness of body ($d$) | | 10 cm | 1 m | 10 m | 100 m | 1 km | 10 km | 100 km |
|---|---|---|---|---|---|---|---|---|
| Cooling timescale ($\sim d^2$/thermal diffusivity) | | 1 hr | 1 d | 1 yr | 10 yr | 10 kyr | 1 Myr | 100 Myr |
| Dominant remanence carriers | $k$ (per cent per OoM) | $\Delta TRM$ (per cent) | | | | | | |
| Ideal SD | ∼ 7 | 5 | 15 | 30 | 40 | 60 | 75 | 90 |
| PSD (and MD) | ∼ 2 | 2 | 4 | 9 | 11 | 17 | 21 | 25 |
| Interacting SD | ∼ 1 | 1 | 2 | 5 | 6 | 9 | 11 | 13 |

make these samples. We are also grateful to David Dunlop and Juan Morales for reviewing this manuscript. AJB undertook this research while funded by an Advanced Fellowship (NE/F015208/1) from the UK's Natural Environment Research Council (NERC). EH is funded by NERC grant NE/I013873/1. ARM was funded by the Royal Society.

## REFERENCES

Biggin, A.J. & Poidras, T., 2006. First-order symmetry of weak-field partial thermoremanence in multi-domain ferromagnetic grains. 1. Experimental evidence and physical implications, *Earth planet. Sci. Lett.*, **245**, 438–453.

Biggin, A.J., Perrin, M. & Dekkers, M.J., 2007. A reliable absolute palaeointensity determination obtained from a non-ideal recorder, *Earth planet. Sci. Lett.*, **257**, 545–563.

Bol'shakov, A.S. & Shcherbakova, V.V., 1979. A thermomagnetic criterion for determining the domain structure of ferrimagnetics, *Izv. Acad. Sci. USSR Phys. Solid Earth*, **15**, 111–117.

Dankers, P.H.M., 1981. Relationship between median destructive field and remanent coercive forces for dispersed natural magnetite, titanomagnetite and hematite, *Geophys. J. R. astr. Soc.*, **64**, 447–461.

Dodson, M.H. & McClelland-Brown, E., 1980. Magnetic blocking temperatures of single-domain grains during slow cooling, *J. geophys. Res.*, **85**, 2625–2637.

Dunlop, D.J. & Özdemir, Ö., 1997. *Rock Magnetism, Fundamentals and Frontiers*, Cambridge University Press, Cambridge.

Dunlop, D.J. & Özdemir, Ö., 2001. Beyond Neel's theories: thermal demagnetization of narrow-band partial thermoremanent magnetizations, *Phys. Earth planet. Inter.*, **126**, 43–57.

Dunlop, D.J., Newell, A.J. & Enkin, R.J., 1994. Transdomain thermoremanent magnetization, *J. geophys. Res.-Solid Earth*, **99**, 19 741–19 755.

Ferk, A., von Aulock, F.W., Leonhardt, R., Hess, K.U. & Dingwell, D.B., 2010. A cooling rate bias in paleointensity determination from volcanic glass: an experimental demonstration, *J. geophys. Res.-Solid Earth*, **115**, B08102, doi:10.1029/2009JB006964.

Ferk, A., Leonhardt, R., Hess, K.U., Koch, S., Krasa, D., Egli, R., Winklhofer, M. & Dingwell, D.B., 2012. Cooling rate dependence of the TRM of SD, PSD and MD particles, in *EGU General Assembly 2012*, Vienna, EGU2012–5244.

Folgerhaiter, G., 1899. Sur les variations séculaires de l'inclinaison magnétique dans l'antiquité, *J. Phys.*, **8**, 660–667.

Fox, J.M.W. & Aitken, M.J., 1980. Cooling-rate dependence of thermoremanent magnetisation, *Nature*, **283**, 462–463.

de Groot, L.V., Dekkers, M.J. & Mullender, T.A.T., 2012. Exploring the potential of acquisition curves of the anhysteretic remanent magnetization as a tool to detect subtle magnetic alteration induced by heating, *Phys. Earth planet. Inter.*, **194**, 71–84.

Halgedahl, S.L., Day, R. & Fuller, M., 1980. The effect of cooling rate on the intensity of weak-field TRM in single-domain magnetite, *J. geophys. Res.*, **85**, 3690–3698.

Harrison, R.J., Dunin-Borkowski, R.E. & Putnis, A., 2002. Direct imaging of nanoscale magnetic interactions in minerals, *Proc. Natl. Acad. Sci. USA*, **99**, 16 556–16 561.

Hartstra, R.L., 1982a. A comparative study of the ARM and Isr of some natural magnetites of MD and PSD grain size, *Geophys. J. R. astr. Soc.*, **71**, 497–518.

Hartstra, R.L., 1982b. Grain-size dependence of initial susceptibility and saturation magnetization-related parameters of 4 natural magnetites in the PSD-MD range, *Geophys. J. R. astr. Soc.*, **71**, 477–495.

Hartstra, R.L., 1983. TRM, ARM and Isr of 2 natural magnetites of MD and PSD grain size, *Geophys. J. R. astr. Soc.*, **73**, 719–737.

Hill, M.J. & Shaw, J., 1999. Palaeointensity results for historic lavas from Mt Etna using microwave demagnetization/remagnetization in a modified Thellier-type experiment, *Geophys. J. Int.*, **139**, 583–590.

Leonhardt, R., Matzka, J., Nichols, A.R.L. & Dingwell, D.B., 2006. Cooling rate correction of paleointensity determination for volcanic glasses by relaxation geospeedometry, *Earth planet. Sci. Lett.*, **243**, 282–292.

McClelland-Brown, E., 1984. Experiments on TRM intensity dependence on cooling rate, *Geophys. Res. Lett.*, **11**, 205–208.

McClelland, E. & Shcherbakov, V.P., 1995. Metastability of domain state in multidomain magnetite: consequences for remanence acquisition, *J. geophys. Res.-Solid Earth*, **100**, 3841–3857.

Morales, J., Goguitchaichvili, A. & Urrutia-Fucugauchi, J., 2006. Cooling rate effects on the magnetization of volcanic rocks: some implications for paleointensity determination, *Geofis. Int.*, **45**, 141–146.

Muxworthy, A., Heslop, D. & Williams, W., 2004. Influence of magnetostatic interactions on first-order-reversal-curve (FORC) diagrams: a micromagnetic approach, *Geophys. J. Int.*, **158**, 888–897.

Muxworthy, A.R. & Dunlop, D.J., 2002. First-order reversal curve (FORC) diagrams for pseudo-single-domain magnetites at high temperature, *Earth planet. Sci. Lett.*, **203**, 369–382.

Muxworthy, A.R. & Heslop, D., 2011. A Preisach method for estimating absolute paleofield intensity under the constraint of using only isothermal measurements: 1. Theoretical framework, *J. geophys. Res.-Solid Earth*, **116**, B04102, doi:10.1029/2010JB007843.

Muxworthy, A.R., Dunlop, D.J. & Williams, W., 2003. High-temperature magnetic stability of small magnetite particles, *J. geophys. Res.-Solid Earth*, **108**(B5), 2281, doi:10.1029/2002JB002195.

Muxworthy, A.R., Heslop, D., Paterson, G.A. & Michalk, D., 2011. A Preisach method for estimating absolute paleofield intensity under the constraint of using only isothermal measurements: 2. Experimental testing. *J. geophys. Res.-Solid Earth*, **116**, B04103, doi:10.1029/2010JB007844.

Néel, L., 1955. Some theoretical aspects of rock magnetism, *Adv. Phys.*, **4**, 191–242.

Papusoi, C., 1972a. Effet de la vitesse de refroidissement sur l'intensité de l'aimantation thermorémanente d'un ensemble de grains monodomaines, *An. Stiint. Univ. Al. I. Cuza Iasi Sect 1b, Tomul*, **18**, 31–47.

Papusoi, C., 1972b. Variation de l'intensité de l'aimantation thermorémanente d'un ensemble de grains à structure de polydomaines magnétiques en fonction de la vitesse de refroidissement, *An. Stiint. Univ. Al. I. Cuza Iasi Sect 1b, Tomul*, **18**, 155–166.

Perrin, M., 1998. Paleointensity determination, magnetic domain structure, and selection criteria, *J. geophys. Res.-Solid Earth*, **103**, 30 591–30 600.

Stancu, A. & Spinu, L., 1998. Temperature- and time-dependent Preisach model for a Stoner-Wohlfarth particle system, *IEEE Trans. Magn.*, **34**, 3867–3875.

Tarduno, J.A. *et al.*, 2010. Geodynamo, solar wind, and magnetopause 3.4 to 3.45 billion years ago, *Science*, **327**, 1238–1240.

Tauxe, L., Bertram, H.N. & Seberino, C., 2002. Physical interpretation of hysteresis loops: micromagnetic modeling of fine particle magnetite, *Geochem. Geophys. Geosyst.*, **3**, 1055, doi:10.1029/2001GC000241.

Thellier, E., 1938. Sur l'aimantation des terres cuites et ses applications géophysique, *Ann. Inst. Phys. Globe Univ. Paris*, **16**, 157–302.

Winklhofer, M., Fabian, K. & Heider, F., 1997. Magnetic blocking temperatures of magnetite calculated with a three-dimensional micromagnetic model, *J. geophys. Res.-Solid Earth*, **102**, 22 695–22 709.

Yu, Y., 2011. Importance of cooling rate dependence of thermoremanence in paleointensity determination, *J. geophys. Res.-Solid Earth*, **116**, B09101, doi:10.1029/2011JB008388.